

Supporting Information for

Assembly and Properties of Heterobimetallic Co^{II/III}/Ca^{II} Complexes with Aquo and Hydroxo Ligands

David C. Lacy,[†] Young Jun Park,[†] Joseph W. Ziller,[†] Junko Yano,[¶] and A. S. Borovik^{†*}

[†]Department of Chemistry, University of California-Irvine, 1102 Natural Sciences II, Irvine, CA 92697; [¶]Physical Biosciences Division, Lawrence Berkeley National Laboratory, Berkeley, CA 94720

E-mail: aborovik@uci.edu

Contents

Crystallography		S2
Table S1		S3
Figure S1	UV-vis spectra of the Co ^{II} complexes	S4
Figure S2a	UV-vis titration for the synthesis of [Co ^{II} (μ-OH ₂)Ca ^{II} OH ₂] ⁺	S4
Figure S2b	FTIR spectra of the Co ^{II} complexes	S4
Figure S3	Cyclic Voltammetry	S5
Figure S4	EPR Spectroscopy of the Co ^{II} complexes	S6
Figure S5	UV-vis spectra of Co ^{III} complexes in TBP symmetry	S7
Figure S6	Molecular structure of [Co ^{III} MST(OH ₂)]	S7
Figure S7	FTIR spectrum of [Co ^{III} (μ-OH)Ca ^{II}] ⁺	S8
Figure S8	UV-vis spectra for the reaction of DPH and [Co ^{III} (μ-OH)Ca ^{II}] ⁺	S8
Figure S9	EPR spectra for the reaction of DPH and [Co ^{III} (μ-OH)Ca ^{II}] ⁺	S9
References		S9

Crystallography

General Methods. Data collections were performed on a Bruker SMART APEX II diffractometer. The APEX2¹ program package was used to determine the unit-cell parameters and for data collection (25 sec/frame scan time for a sphere of diffraction data unless otherwise stated). The raw frame data were processed using SAINT² and SADABS³ to yield the reflection data files. Subsequent calculations were carried out using the SHELXTL⁴ program. The analytical scattering factors⁵ for neutral atoms were used throughout the analyses. The structures were solved by direct methods and refined on F² by full-matrix least-squares techniques.

Structure of Me₄N[Co^{II}MST]. A blue crystal of approximate dimensions 0.09 x 0.22 x 0.37 mm was mounted on a glass fiber. The diffraction symmetry was 2/m and the systematic absences were consistent with the monoclinic space group P2₁/n that was later determined to be correct. Hydrogen atoms were included using a riding model. At convergence, wR2 = 0.0886 and Goof = 1.035 for 482 variables refined against 10021 data (0.74Å), R1 = 0.0335 for those 8583 data with I > 2.0σ(I).

Structure of Me₄N[Co^{II}MST(OH₂)]. A purple crystal of approximate dimensions 0.04 x 0.19 x 0.47 mm was mounted on a glass fiber (30 sec/frame scan time for a sphere of diffraction data). The diffraction symmetry was 2/m and the systematic absences were consistent with the monoclinic space groups Cc and C2/c. It was later determined that space group C2/c was correct. Hydrogen atoms H(1) and H(2) were located from a difference-Fourier map and refined (x,y,z and U_{iso}). The remaining hydrogen atoms were included using a riding model. Carbon atoms C(35)-C(37) were disordered and included using multiple components with partial site-occupancy-factors. Carbon atom C(34) was refined as two components with identical constrained coordinates and thermal parameters (EXYZ and EADP)⁴. At convergence, wR2 = 0.0853 and Goof = 1.028 for 531 variables refined against 9573 data (0.74Å), R1 = 0.0328 for those 8063 data with I > 2.0σ(I).

Structure of [Co^{II}MST(μ-OH₂)Ca^{II}c15crown5-(OH₂)]OTf. A pink crystal of approximate dimensions 0.12 x 0.17 x 0.47 mm was mounted on a glass fiber (20 sec/frame scan time for a sphere of diffraction data). There were no systematic absences or any diffraction symmetry other than the Friedel condition. The centrosymmetric triclinic space group P-1 was assigned and later determined to be correct. Hydrogen atoms H(1), H(2), H(13C) and H(13D) were located from a difference-Fourier map and refined (x,y,z and U_{iso}) with d(O-H) = 0.85Å. The remaining hydrogen atoms were included using a riding model. Least-squares analysis yielded wR2 = 0.1387 and Goof = 1.080 for 683 variables (4 restraints) refined against 13265 data (0.74Å), R1 = 0.0461 for those 11313 data with I > 2.0σ(I). There were several high residuals present in the final difference-Fourier map. It was not possible to determine the nature of the residuals although it is probable that dichloromethane solvent was present. The SQUEEZE routine in the PLATON⁶ program package was used to account for the electrons in the solvent accessible voids.

Structure of [Co^{III}MST(μ-OH)Ca^Ic15crown5]OTf•DCM. A brown crystal of approximate dimensions 0.09 x 0.24 x 0.34 mm was mounted on a glass fiber. There were no systematic absences or any diffraction symmetry other than the Friedel condition. The centrosymmetric triclinic space group P-1 was assigned and later determined to be correct. Hydrogen atoms were either located from a difference-Fourier map and refined (x,y,z and U_{iso}) or were included using a riding model (mixed refinement). There was one molecule of dichloromethane solvent present. At convergence, wR2 = 0.0996 and Goof = 1.035 for 937 variables refined against 13276 data (0.74Å), R1 = 0.0346 for those 11430 data with I > 2.0σ(I).

Structure of [Co^{III}MST(OH₂)]•DCM. An orange crystal of approximate dimensions 0.04 x 0.10 x 0.29 mm was mounted on a glass fiber (60 sec/frame scan time for a sphere of diffraction data). There were no systematic absences nor any diffraction symmetry other than the Friedel condition. The centrosymmetric triclinic space group P-1 was assigned and later determined to be correct. Hydrogen atoms H(1) and H(2) were located from a difference-Fourier map and refined (x,y,z and

U_{iso}). The remaining hydrogen atoms were included using a riding model. There was one molecule of dichloromethane solvent present. At convergence, wR2 = 0.0894 and Goof = 1.016 for 477 variables refined against 9099 data (0.75Å), R1 = 0.0382 for those 6795 data with I > 2.0σ(I).

Table 1. Crystal data and structure refinement for the Co-MST complexes.

	Me ₄ N[Co ^{II} MST]	Me ₄ N[Co ^{II} MST(OH ₂)]	[Co ^{II} (μ-OH ₂)Ca ^{II} (OH ₂)OTf]	[Co ^{III} MST(OH ₂)]•CH ₂ Cl ₂	[Co ^{III} (μ-OH)Ca ^{II}]OTf•CH ₂ Cl ₂
formula	C ₃₇ H ₃₇ CoN ₅ O ₆ S ₃	C ₃₇ H ₃₉ CoN ₅ O ₇ S ₃	C ₄₄ H ₆₉ CaCoF ₃ N ₄ O ₁₆ S ₄	C ₃₃ H ₄₇ CoN ₄ O ₇ S ₃ •CH ₂ Cl ₂	C ₄₅ H ₆₈ CaCl ₂ CoF ₃ N ₄ O ₁₆ S ₄
FW	822.99	841.00	1194.28	851.78	1260.18
T (K)	88(2)	143(2)	88(2)	88(2)	88(2)
crystal system	Monoclinic	Monoclinic	Triclinic	Triclinic	Triclinic
space group	<i>P</i> 2 ₁ / <i>n</i>	<i>C</i> 2/ <i>c</i>	<i>P</i> -1	<i>P</i> -1	<i>P</i> -1
<i>a</i> (Å)	21.1381(8)	26.5997(15)	9.4438(4)	7.6668(4)	11.2366(6)
<i>b</i> (Å)	9.0319(3)	9.6741(5)	17.4810(7)	14.8717(8)	15.2439(7)
<i>c</i> (Å)	21.2593(8)	31.4984(18)	17.5309(7)	17.4049(9)	17.5369(9)
α (deg)	90	90	73.4591(4)	92.5600(7)	71.8050(6)
β (deg)	95.0347(4)	90.3563(6)	88.5336(4)	96.5047(7)	84.3928(6)
γ (deg)	90	90	85.2907(5)	101.7540(7)	77.3591(6)
Z	4	8	2	2	2
V (Å ³)	4043.1(3)	8105.3(8)	2765.0(2)	1925.67(18)	2783.1(2)
d _{calcd} (Mg/m ³)	1.352	1.378	1.434	1.469	1.504
Indep. Reflections	10021	9573	13265	9099	13276
R1	0.0335	0.0328	0.0461	0.0382	0.0346
wR2	0.084	0.0803	0.1336	0.0799	0.0945
GOF	1.035	1.028	1.08	1.016	1.035

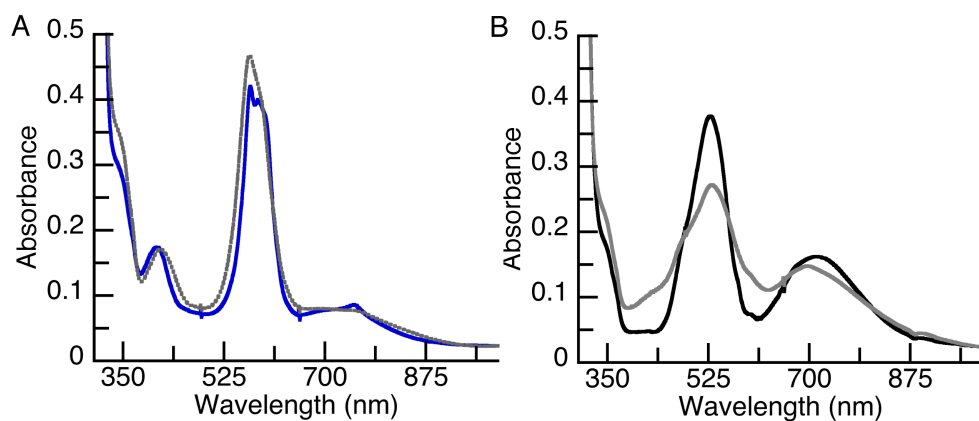


Figure S1. (A) UV-vis spectrum of $[\text{Co}^{\text{II}}\text{MST}]^-$ (blue) and after the addition of 1 equiv $\text{Ca}(\text{OTf})_2/15\text{-crown-5}$ (dotted grey). (B) UV-vis spectrum of $[\text{Co}^{\text{II}}\text{MST}(\text{OH}_2)]^-$ (black) and $[\text{Co}^{\text{II}}(\mu\text{-OH}_2)\text{Ca}^{\text{II}}\text{OH}_2]^+$ (grey). Conditions: ~ 10 mM, DCM, 1 cm path length cell.

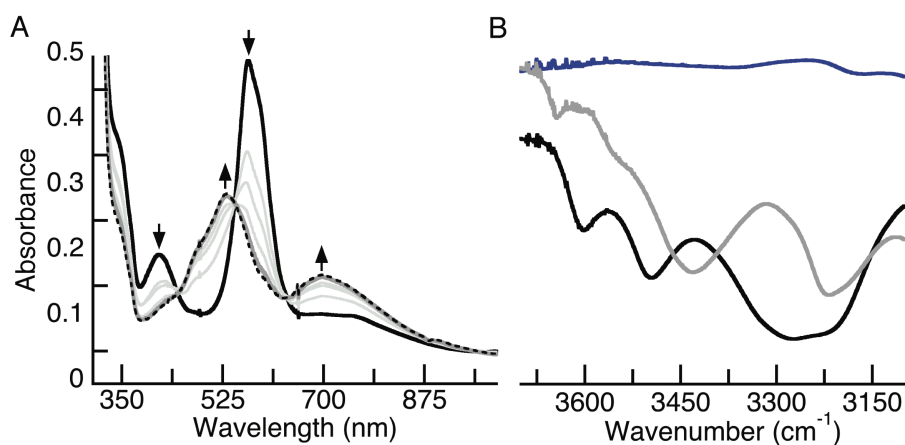


Figure S2. (A) The titration of a mixture of 0.5 mM $[\text{Co}^{\text{II}}\text{MST}]^-$ (DCM) and 1 equiv $\text{Ca}(\text{OTf})_2/15\text{-crown-5}$ (black) with water was followed by UV-vis spectroscopy in a 1 cm cuvette. The light grey lines correspond to 0.33, 0.50, 0.66, and 1.00 (dark grey) and up to 1000 equiv (dashed black line) of water. (B) FTIR spectra of the νOH region for $\text{Me}_4\text{N}[\text{Co}^{\text{II}}\text{MST}]$ (blue), $\text{Me}_4\text{N}[\text{Co}^{\text{II}}\text{MST}(\text{OH}_2)] \cdot 2\text{H}_2\text{O}$ (black) and $[\text{Co}^{\text{II}}(\mu\text{-OH}_2)\text{Ca}^{\text{II}}\text{OH}_2]\text{OTf}$ (grey).

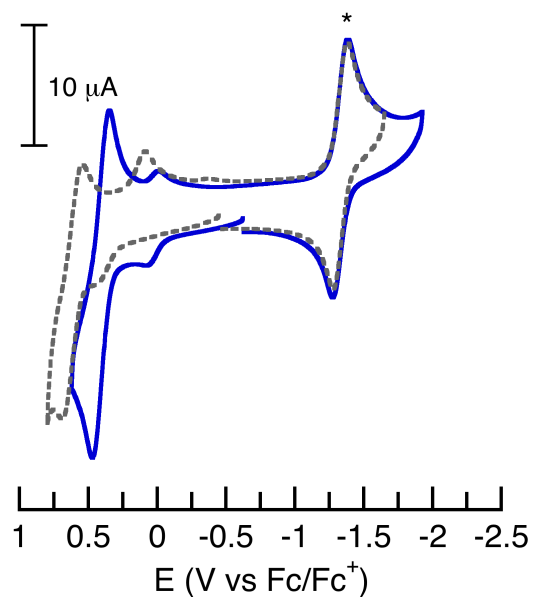


Figure S3. Cyclic voltammograms of $[Co^{II}MST]^-$ (solid blue) and after the addition of 1 equiv $Ca(OTf)_2/15$ -crown-5 (dashed grey). Cobaltocenium (*) was used as an internal reference. Scan rate 0.1 V/s; solvent, DCM; electrolyte, 100mM TBAP; analyte, 1mM complex at rt; working electrode, glassy carbon; reference electrode, silver wire; counter electrode, platinum wire.

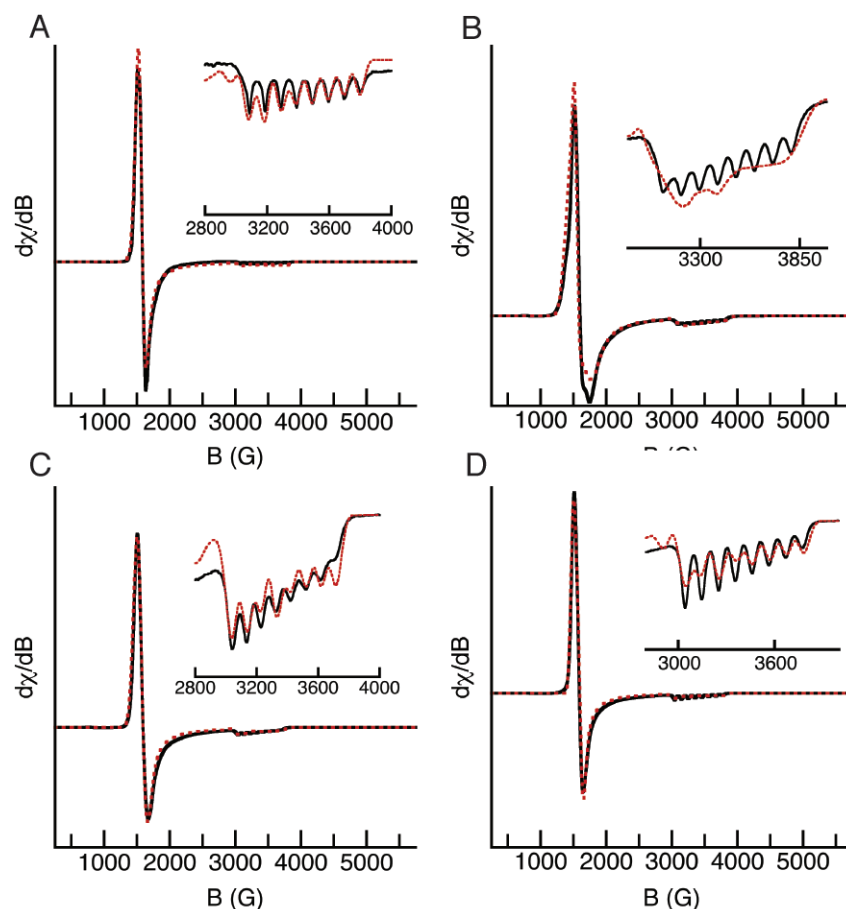


Figure S4. EPR spectra (black) and simulations (dashed red) of $[\text{Co}^{\text{II}}\text{MST}]^-$ (A), simulation parameters: $D = 2$, $E/D = 0.010$, $g_x = 2.247$, $g_y = 2.210$, $g_z = 2.004$, $A_z = 96 \times 10^{-4} \text{ cm}^{-1}$; $[\text{Co}^{\text{II}}\text{MST}]^- + \text{Ca}(\text{OTf})_2/15\text{-crown-5}$ (B), simulation parameters: $D = 2 \text{ cm}^{-1}$, $E/D = 0.049$, $g_x = 2.230$, $g_y = 2.252$, $g_z = 2.000$, $A_z = 94 \times 10^{-4} \text{ cm}^{-1}$; $[\text{Co}^{\text{II}}\text{MST}(\text{OH}_2)]^-$ (C), simulation parameters: $D = 2 \text{ cm}^{-1}$, $E/D = 0.0236$, $g_x = 2.315$, $g_y = 2.157$, $g_z = 2.0437$, $A_z = 90 \times 10^{-4} \text{ cm}^{-1}$; $[\text{Co}^{\text{II}}(\mu\text{-OH}_2)\text{Ca}^{\text{II}}\text{OH}_2]^+$ (D), simulation parameters: $D = 2 \text{ cm}^{-1}$, $E/D = 0.030$, $g_x = 2.248$, $g_y = 2.210$, $g_z = 2.0252$, $A_z = 98 \times 10^{-4} \text{ cm}^{-1}$. All samples were prepared to be 6mM in concentration in DCM and recorded at 10K with the following experimental parameters: frequency 9.64 GHz, power 0.20 mW, modulation amplitude 9.02 G, time constant 20.48 s, conversion time 40.96 s. Inset show zoomed in view of the hyperfine structure and simulation.

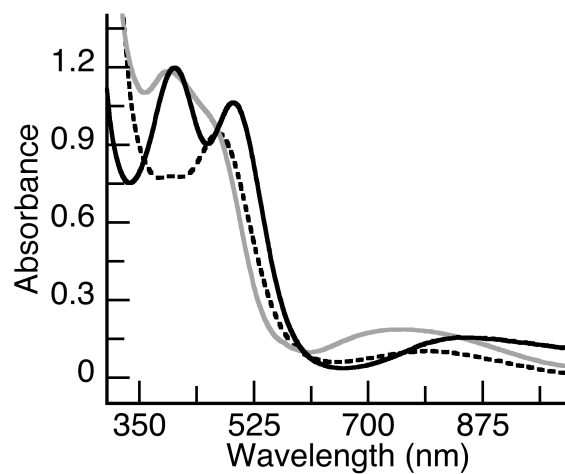


Figure S5. UV-vis spectra of $[\text{Co}^{\text{III}}\text{H}_3\text{buea}(\text{OH})]^-$ (dashed black, DMA, 0.2 M, rt), $[\text{Co}^{\text{III}}\text{MST}(\text{OH}_2)]$ (solid black, DCM, 0.2 M), and $[\text{Co}^{\text{III}}(\mu\text{-OH})\text{Ca}^{\text{II}}]^+$ (solid grey, DCM, 0.2 M). The $[\text{Co}^{\text{III}}\text{H}_3\text{buea}(\text{OH})]^-$ complex was synthesized using literature procedures.⁷

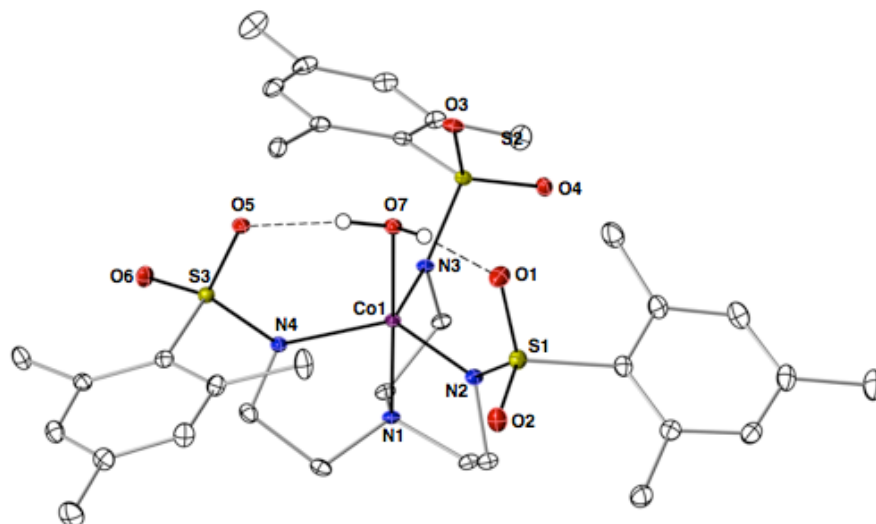


Figure S6. Thermal ellipsoid diagram depicting the molecular structure of $[\text{Co}^{\text{III}}\text{MST}(\text{OH}_2)]$. The thermal ellipsoids are drawn at the 50% probability level and only the hydrogen atoms of the aquo ligand are shown for clarity.

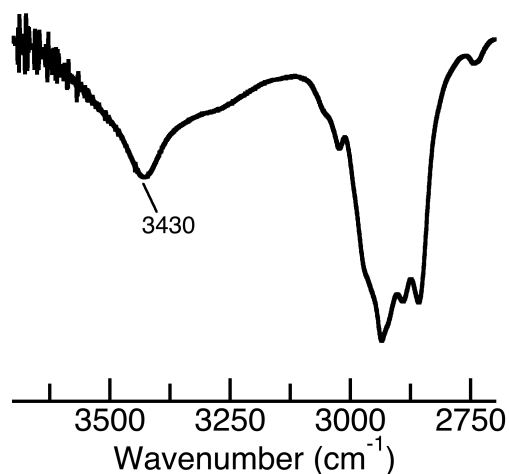


Figure S7. FTIR spectrum of a KBr pellet of $[\text{Co}^{\text{III}}(\mu\text{-OH})\text{Ca}^{\text{II}}]\text{OTf}$ showing the strong $\nu(\text{OH})$ at 3430 cm^{-1} .

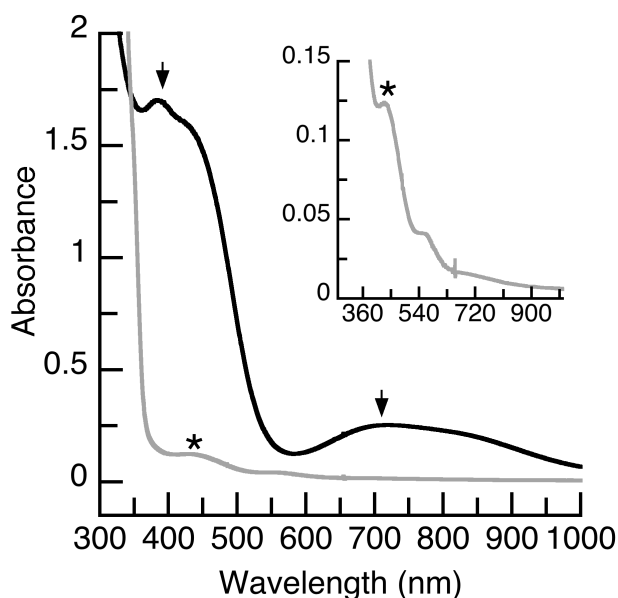


Figure S8. UV-vis spectrum of $[\text{Co}^{\text{III}}(\mu\text{-OH})\text{Ca}^{\text{II}}]^+$ before (black) and 22 min after the addition of DPH (grey): the inset is a zoomed in view of the grey line (azobenzene (*)). Conditions: A solution of $[\text{Co}^{\text{III}}(\mu\text{-OH})\text{Ca}^{\text{II}}]^+$ (4 mL, $400\text{ }\mu\text{M}$) was treated with a DCM solution of DPH ($80\text{ }\mu\text{L}$, 0.29 M , $\sim 10\text{-}20$ equiv) and allowed to react in a 1 cm cuvette at 20°C . The yield of azobenzene was 70% (based on unreacted DPH) determined by performing the experiment with $[\text{Co}^{\text{III}}(\mu\text{-OH})\text{Ca}^{\text{II}}]^+$ (1 mL, 5 mM) and DPH (9.2 mg, 0.05 mmol) in $\text{DCM-}d_2$ with toluene as an internal standard.

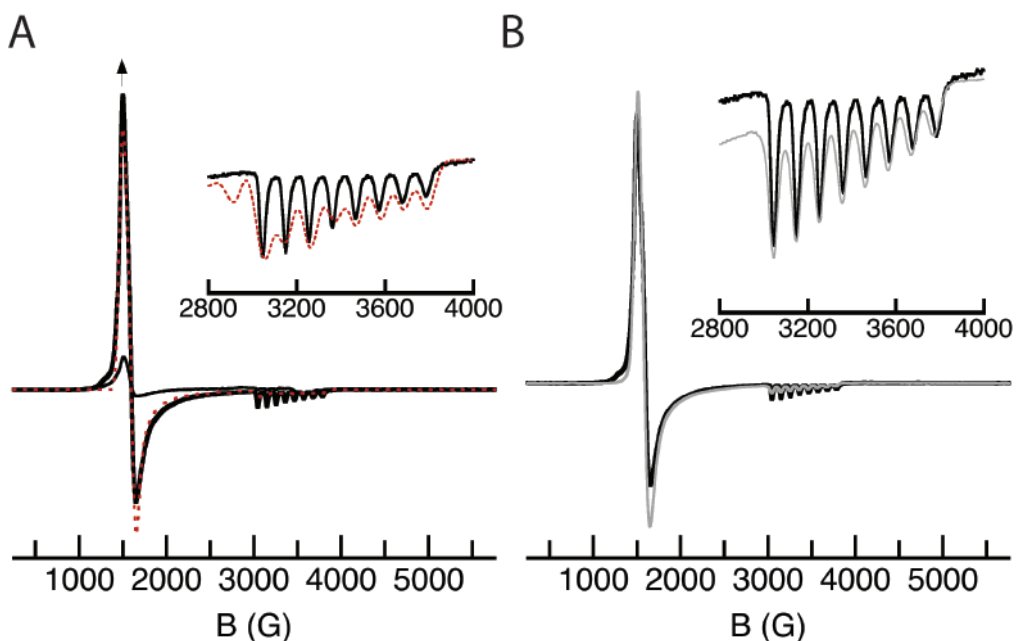


Figure S9. (A) EPR spectrum of $[\text{Co}^{\text{III}}(\mu\text{-OH})\text{Ca}^{\text{II}}]^+$ before and after treatment with 10 equiv DPH (black). The product of the reaction was simulated (dashed red) using the same parameters used to simulate $[\text{Co}^{\text{II}}(\mu\text{-OH}_2)\text{Ca}^{\text{II}}\text{OH}_2]^+$ (Figure S4D). (B) For comparison, the EPR spectra of $[\text{Co}^{\text{II}}(\mu\text{-OH}_2)\text{Ca}^{\text{II}}\text{OH}_2]^+$ (grey) is overlaid with the product of the reaction between $[\text{Co}^{\text{III}}(\mu\text{-OH})\text{Ca}^{\text{II}}]^+$ and DPH (black). Experimental conditions are the same as used in Figure S4. Inset show a zoomed in view of the $g = 2$ region.

References

1. APEX2 Version 2010.9-1, Bruker AXS, Inc.; Madison, WI 2010.
2. SAINT Version 7.68a, Bruker AXS, Inc.; Madison, WI 2009.
3. Sheldrick, G. M. SADABS, Version 2008/1, Bruker AXS, Inc.; Madison, WI 2008.
4. Sheldrick, G. M. SHELXTL, Version 2008/4, Bruker AXS, Inc.; Madison, WI 2008.
5. International Tables for X-Ray Crystallography **1992**, Vol. C., Dordrecht: Kluwer Academic Publishers.
6. Spek, A. L. PLATON, Acta. Cryst. **2009**, D65, 148-155
7. Hammes, B. S.; Young, Jr. G. V.; Borovik, A. S. *Angew. Chem. Int. Ed.* **1999**, 38, 666-669.